Do B3LYP and CCSD(T) Predict Different Hydrosilylation Mechanisms? Influences of Theoretical Methods and Basis Sets on Relative Energies in Ruthenium−Silylene-Catalyzed Ethylene Hydrosilylation

Chad Beddie and Michael B. Hall*

Department of Chemistry, Texas A&M University, P.O. Box 30012, College Station, TX, 77842-3012

Received: August 16, 2005; In Final Form: October 3, 2005

A series of density functional theory (DFT) and wave function theory (WFT) methods were used in conjunction with a series of basis sets to investigate the influence of the computational methodology on the relative energies of key intermediates and transition states in potential reaction pathways in ruthenium−silylene-catalyzed hydrosilylation reactions. A variety of DFT methods in a modest basis set and B3LYP calculations in a variety of basis sets calculated the key transition in the Glaser−Tilley (GT) pathway to be energetically favored. In contrast, with the smaller basis sets, the CCSD(T) method calculated the Chalk−Harrod (CH) pathway to be favored; however, CCSD(T) results extrapolated to larger basis sets favored the GT pathway.

I. Introduction

Hydrosilylation reactions are widely used for the addition of Si−H bonds across C−C, C−N, and C−O multiple bonds in organic synthesis and organosilicon, polymer, and dendrimer chemistry; thus, hydrosilylation reactions have been studied extensively.[1−5] Recently, Glaser and Tilley (GT) developed a cationic ruthenium−silylene catalyst capable of facilitating highly regioselective anti-Markovnikov hydrosilylation of alkenes (Scheme 1).[6]

The GT ruthenium−silylene catalyst system displayed several unusual properties, including the ability to perform hydrosilylation on highly substituted alkenes such as 1-methylcyclohexene, high selectivity for primary silanes over secondary and tertiary silanes, and an absence of unsaturated side-products in the reaction mixture.[6] To account for these observations, Glaser and Tilley proposed a new mechanism in which the key step is alkene insertion into a silicon−hydrogen bond located in a position remote from the metal center.[6] This mechanism is unlike any other proposed for late transition-metal-catalyzed hydrosilylation, since, in all other commonly accepted proposals, both silane and olefin coordinate to the transition metal.[7,8] Since the identification of a new hydrosilylation mechanism has important ramifications for the design of new hydrosilylation catalysts and potential applicability for the design of new catalytic processes,[9] we investigated the catalytic hydrosilylation of alkenes by cationic ruthenium−silylene complexes using a model system consisting of $[(Cp)(PH_3)Ru(H)_2(SiH_2)]^+$, SiH_4, and C_2H_4 with the B3LYP density functional theory (DFT) method with a relatively small basis set (BS1).[10] These investigations indicated that the mechanism proposed by Glaser and Tilley for the formation of the Si−C and C−H bonds is favored in terms of relative electronic energy by over 6.5 kcal/mol and in terms of gas-phase relative free energy by over 8 kcal/mol compared to the lowest energy Chalk−Harrod (CH) and modified Chalk−Harrod (mCH) mechanisms at the B3LYP/BS1 level of theory, and furthermore, served as the first theoretical evidence for this exciting mechanistic proposal.[10] It should be noted that the lowest energy CH and mCH pathways both involve the same high energy transition state for the oxidative addition of SiH_4 to Ru; however, after this point, the CH mechanism is favored over the mCH mechanism at the B3LYP/BS1 level of theory; thus this work focuses on a comparison of the CH mechanism and the GT mechanism.

SCHEME 1. Alkene Hydrosilylation Catalyzed by a Cationic Ruthenium−Silylene Complex.

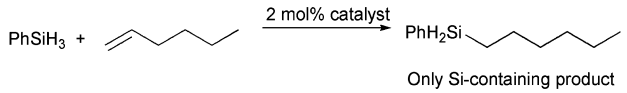

catalyst = $[(C_5Me_5)(i\text{-}Pr_3P)Ru(H)_2(SiHPh)OEt_2][B(C_6F_5)_4]$

As part of our ongoing interest in evaluating and comparing computational methods using transition metal systems,[11−13] we sought to determine whether the conclusion that the GT mechanism is energetically favored was influenced by the computational methodology. To this end, the key reaction steps that determine whether Si−C and C−H bond formation occurs via the GT mechanism or the CH mechanism were examined using a series of DFT and wave function theory (WFT) methods. With BS1, all of the DFT methods tested herein calculated the key transition state in the GT mechanism to be lower in electronic energy than the key transition state in the CH mechanism by at least 6.5 kcal/mol. In contrast, however, with BS1, CCSD(T)[14,15] calculated the energy of the transition state in the GT mechanism to have an electronic energy 3.7 kcal/mol *higher* than the energy of transition state in the CH mechanism.[16] This result revealed a 10 kcal/mol discrepancy between the CCSD(T)/BS1 calculations and all of the DFT/BS1 calculations. Although it is well-known that small basis set CCSD(T) calculations are not particularly accurate, these results raise the question, Does the CCSD(T) method predict that the CH pathway is energetically favored over the GT pathway?

To investigate these contradictory results, B3LYP, HF, MP2, MP3, MP4SDQ, CISD, CCSD, and CCSD(T) calculations were conducted with a series of larger basis sets, and the results are discussed in detail in this report. The basis set testing suggests

* Corresponding author. E-mail: hall@science.tamu.edu.

10.1021/jp054622o CCC: $33.50
Published on Web 12/10/2005

TABLE 1: Basis Sets Used in This Investigation

	Ru[a,b,c]	P, Si	C	H from C_2H_4 and SiH_4	H from PH_3 and C_5H_5
BS1	LANL2DZ + Couty−Hall 5p	LANL2DZdp	6-31G(d′)	6-31G(d′,p′)	6-31G
BS2	LANL2TZ* + Couty−Hall 5p + f	LANL2DZdp	6-31++G(d′,p′)	6-31++G(d′,p′)	6-31++G(d′,p′)
BS3	Stuttgart 1997 ECP + f	LANL2DZdp	6-31G(d′)	6-31G(d′,p′)	6-31G
BS4	Stuttgart 1997 ECP + f	LANL2DZdp	6-31++G(d′,p′)	6-31++G(d′,p′)	6-31++G(d′,p′)
BS5	Stuttgart 1997 ECP + f	cc-pVDZ	cc-pVDZ	cc-pVDZ	cc-pVDZ
BS6	Stuttgart 1997 ECP + f	cc-pVTZ	cc-pVTZ	cc-pVTZ	cc-pVTZ
BS7[d]	Stuttgart 1997 ECP + f	cc-pV#Z	cc-pV#Z	cc-pV#Z	cc-pV#Z

[a] Couty−Hall 5p indicates that reoptimized 5p orbitals were used for Ru. [b] LANL2TZ* indicates that the d orbitals were split to triple-ζ. [c] + f indicates that f-polarization functions with an exponent of 1.235 were used for Ru (see ref 22). [d] BS7 is a hypothetical basis set in which the basis set for Ru is the Stuttgart 1997 ECP + f and the basis sets for P, Si, C, and H are extrapolated as described in the text.

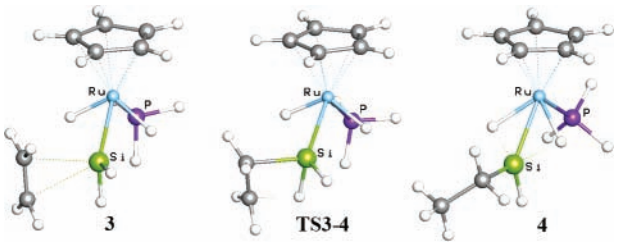

Figure 1. Key structures in the Glaser−Tilley (GT) mechanism.

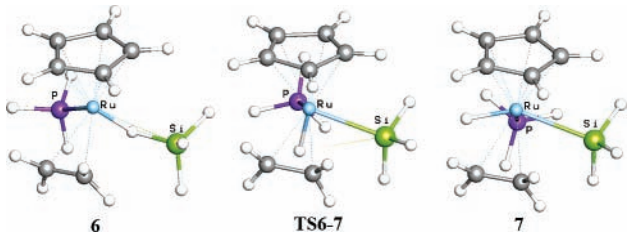

Figure 2. Key structures in the Chalk−Harrod (CH) mechanism.

that, for large basis sets, all of the methods except for MP2 and MP4SDQ predict that the energy of the GT transition state (**TS3-4**) is lower than the energy of the CH transition state (**TS6-7**).

II. Computational Details

All calculations were performed using the Gaussian 03 suite of programs.[17] Optimized gas-phase geometries were obtained using the B3LYP method,[18,19] as implemented in Gaussian 03. The basis sets used for geometry optimizations (BS1) and energy calculations (BS1, BS2, BS3, BS4, BS5, BS6, and BS7) were implemented as described in Table 1.

Basis sets 1−6 were constructed using various combinations of basis sets for Ru, P, Si, C, and H (Table 1). The three Ru basis sets used to construct basis sets 1−6 were (1) LANL2DZ + Couty−Hall 5p, in which a set of optimized 5p orbitals[20] supplement the LANL2DZ basis set;[21] (2) LANL2TZ* + Couty−Hall 5p + f, which differs from LANL2DZ + Couty−Hall 5p in that the LANL2DZ valence d-orbitals were decontracted to triple-ζ, and f-polarization functions[22] were added; and (3) Stuttgart 1997 ECP + f, in which the Stuttgart, relativistic, small core effective core potential basis set[23,24] was supplemented with f-polarization functions.[22] For Si, P, C, and H, the following basis sets were used to construct basis sets 1−6: (1) LANL2DZdp;[21,24,25] (2) cc-pVDZ;[26,27] (3) cc-pVTZ;[26,27] (4) 6-31G;[28] (5) 6-31G(d′);[29−33] and (6) 6-31++G(d′,p′).[28−34] BS7 is a hypothetical basis set in which the basis set for Ru is the Stuttgart 1997 ECP + f and the basis sets for P, Si, C, and H are extrapolated.

Calculating the harmonic vibrational frequencies at the B3LYP/BS1 level of theory and noting the number of imaginary frequencies (NImag) confirmed the nature of all intermediates (NImag = 0) and transition state structures (NImag = 1). Single-point calculations at B3LYP/BS1 geometries were used to calculate relative energies with the DFT methods B3PW91,[18,35] MPWPW91,[35,36] MPW1PW91,[35,36] OLYP,[19,37] O3LYP,[38] PBEPBE,[39] and PBE1PBE,[39] and the WFT methods HF,[40] MP2,[41,42] MP3,[43,44] MP4SDQ,[45] CISD,[44,46] CCSD,[14] and CCSD(T).[15] Relative energies are reported in kcal mol^{-1}.

Representations of the intermediates and transitions states shown in Figures 1 and 2 were created using the JIMP software program.[47]

TABLE 2: Gas-Phase Relative Energies (kcal/mol) of the Intermediates and Transition States in the GT and CH Hydrosilylation Pathways at the B3LYP/BS1 Level of Theory

structure	ΔE_e[a]	ΔE_0[b]	$\Delta H°$[c]	$\Delta G°$[d]
		GT mechanism		
1 + C_2H_4	0.00	0.0	0.0	0.0
2	−6.41	−5.3	−5.1	3.8
TS2−3	−6.36	−5.6	−5.9	4.6
3	−8.50	−6.7	−6.8	3.9
TS3−4	−0.16	1.9	0.9	13.8
4	−38.00	−33.7	−34.2	−22.8
		CH mechanism		
1 + C_2H_4	0.00	0.0	0.0	0.00
5	−3.38	−2.8	−2.1	3.9
TS5−6	4.42	5.1	5.5	14.7
6	−16.95	−13.8	−14.1	−2.2
TS6−7	6.50	9.3	8.4	22.4
7	−12.34	−8.6	−9.4	4.0
TS7−8	−12.15	−9.1	−10.1	3.8
8	−17.59	−12.9	−13.8	−0.1
TS8−9	−5.99	−1.6	−2.5	10.8
9	−24.53	−20.0	−20.4	−8.7

[a] Based on the gas-phase relative electronic energy of **1** + C_2H_4 set to 0.00 kcal/mol. [b] Based on the gas-phase relative zero-point corrected energy of **1** + C_2H_4 set to 0.0 kcal/mol. [c] Based on the gas-phase relative enthalpy of **1** + C_2H_4 set to 0.0 kcal/mol. [d] Based on the gas-phase relative free energy of **1** + C_2H_4 set to 0.0 kcal/mol.

III. Results and Discussion

A. The GT and CH Hydrosilylation Mechanisms. Our previous work on ruthenium−silylene-catalyzed hydrosilylation at the B3LYP/BS1 level of theory (Table 2) revealed that the two lowest energy pathways, in terms of the gas-phase relative energies, were the GT pathway (Scheme 2) and the CH pathway (Scheme 3).[10] In the GT pathway (Scheme 2), coordination of ethylene to the cationic ruthenium complex **1** (0.0 kcal/mol) generates the ethylene π complex, **2** (−6.4 kcal/mol), in which ethylene is weakly bound to Si. From **2**, the ethylene moves closer to the Si atom via **TS2−3** (−6.4 kcal/mol) to form another ethylene π complex, **3** (−8.5 kcal/mol), in which ethylene is bound more closely to Si. From **3**, ethylene inserts into the Si−H bond via **TS3−4** (−0.2 kcal/mol) to generate the insertion product **4** (−38.0 kcal/mol), in which the new Si−C and C−H bonds have formed. From **4**, the catalytic cycle is completed

SCHEME 2. Glaser−Tilley (GT) Pathway.[a]

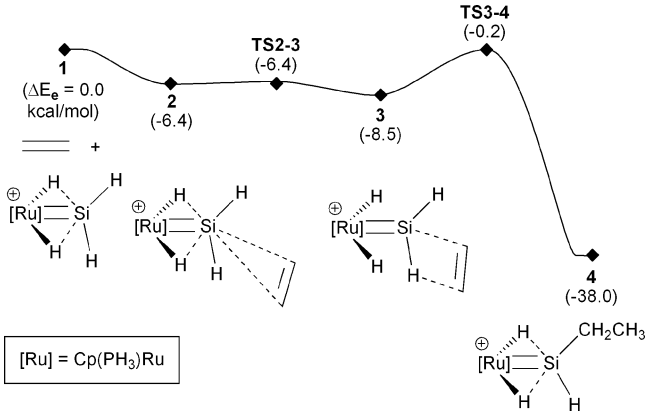

[a] Gas-phase relative electronic energies at the B3LYP/BS1 level of theory based on the energy of separated **1** and C_2H_4 set to 0.0 kcal/mol are provided in parentheses in kcal/mol. Electronic energies, zero-point corrected energies, enthalpies, and free energies are provided in Table 2.

SCHEME 3. Chalk−Harrod (CH) Pathway.[a]

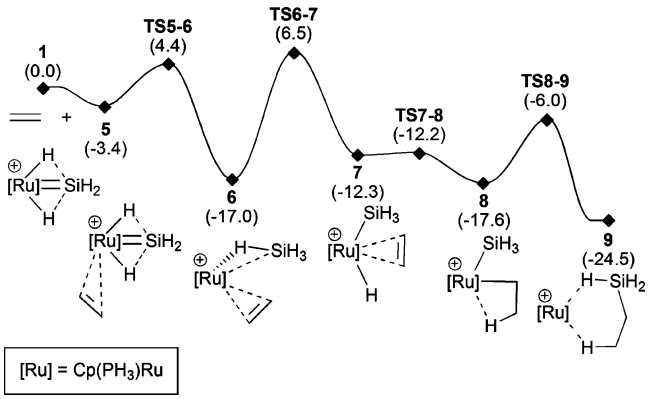

[a] Gas-phase relative electronic energies at the B3LYP/BS1 level of theory based on the energy of separated **1** and C_2H_4 set to 0.0 kcal/mol are provided in parentheses in kcal/mol. Electronic energies, zero-point corrected energies, enthalpies, and free energies are provided in Table 2.

through the release of $H_3SiCH_2CH_3$ and the regeneration of the starting metal complex **1** via a multistep associative displacement mechanism in which SiH_4 coordinates to the Ru center and $H_3SiCH_2CH_3$ is subsequently released.[10]

In the CH pathway (Scheme 3), ethylene coordination to **1** generates an ethylene complex, **5** (−3.4 kcal/mol), in which ethylene is very weakly bound to the Ru. From **5**, ethylene coordinates to the Ru center via **TS5**−**6** (4.4 kcal/mol) to generate **6** (−17.0 kcal/mol), in which SiH_4 is coordinated to the Ru through a σ-complex interaction, and ethylene is tightly bound to Ru. From **6**, oxidative addition of the Si−H bond via **TS6**−**7** (6.5 kcal/mol) generates the hydride complex **7** (−12.3 kcal/mol), in which H and SiH_3 ligands are on opposite sides of the bound ethylene. From **7**, the new C−H bond forms via **TS7**−**8** (−12.2 kcal/mol) to generate **8** (−17.6 kcal/mol), in which the new ethyl ligand contains a β-agostic interaction with the Ru. From **8**, the new Si−C bond forms via **TS8**−**9** (−6.0 kcal/mol) to generate **9** (−24.5 kcal/mol), in which the hydrosilylation product is bound to Ru through σ-complex interactions with Si−H and C−H bonds. From **9**, rearrangement of the $H_3SiCH_2CH_3$ fragment through a series of intermediates and transition states generates the same product species as that from the GT mechanism (**4**), from which the release of $H_3SiCH_2CH_3$ and the regeneration of the starting metal complex **1** occur, as described previously.[10]

TABLE 3: Gas-Phase Relative Electronic Energies (kcal/mol) of the Key Intermediates and Transition State Structures in the GT and CH Pathways Calculated Using BS1 at B3LYP/BS1 Geometries with the Relative Electronic Energy of 3 Set to 0.00 kcal/mol

	GT pathway			CH pathway			TS
method	**3**	**TS3−4**	**4**	**6**	**TS6−7**	**7**	diff.[a]
			DFT methods				
B3LYP	0.00	8.34	−29.50	−8.45	15.00	−3.84	6.66
B3PW91	0.00	5.33	−29.78	−7.30	13.67	−5.38	8.34
OLYP	0.00	4.39	−28.83	−4.63	12.72	−3.05	8.33
O3LYP	0.00	3.33	−30.05	−6.44	11.82	−5.86	8.49
MPWPW91	0.00	3.84	−26.24	−6.15	10.45	−5.85	6.61
MPW1PW91	0.00	5.27	−30.62	−8.00	13.72	−6.10	8.45
PBEPBE	0.00	3.25	−26.26	−6.13	9.84	−6.50	6.58
PBE1PBE	0.00	4.73	−30.58	−7.92	13.20	−6.64	8.46
			WFT methods				
HF	0.00	16.71	−44.17	−16.82	32.22	0.45	15.51
MP2	0.00	8.55	−16.46	−7.30	−7.99	−17.93	−16.54
MP3	0.00	11.28	−32.50	−12.38	22.54	−4.67	11.26
MP4SDQ	0.00	11.34	−22.77	−11.59	−5.44	−14.61	−16.78
CISD	0.00	13.28	−37.12	−15.28	19.54	−6.07	6.26
CCSD	0.00	11.01	−29.73	−13.46	9.93	−9.41	−1.08
CCSD(T)	0.00	10.22	−27.21	−13.72	6.53	−11.34	−3.70

[a] TS diff. = [*E*(**TS6**−**7**) − *E*(**TS3**−**4**)] (kcal/mol).

Basis set superposition error (BSSE) can cause apparent increases in the binding energy between two units through each unit using unused basis functions from the opposing unit to augment its basis set and lower the energy of each unit relative to a calculation of each unit alone.[48] In the GT and CH pathways above, BSSE may be destabilizing the initial reactants **1** + C_2H_4 relative to the rest of the structures in the pathways. The magnitude of the BSSE can be estimated using the counterpoise correction.[49] In the first step of the GT mechanism (**1** + C_2H_4 → **2**) and the CH mechanism (**1** + C_2H_4 → **5**), the BSSE at the B3LYP/BS1 level of theory, as calculated using the counterpoise correction, is 1.90 and 1.35 kcal/mol, respectively. Fortunately, the remainder of this paper focuses on the relative energies of structures **3**, **TS3**−**4**, **4**, **6**, **TS6**−**7**, and **7**, all of which include the same number of atoms and basis functions in each calculation. Therefore, BSSE is not expected to dramatically influence the energies of **3**, **TS3**−**4**, **4**, **6**, **TS6**−**7**, and **7** relative to each other. Furthermore, the relative electronic energies in Tables 3 and 4 were adjusted to set the relative electronic energy of **3** to 0.00 kcal/mol.

B. Influence of Theoretical Method on the Highest Energy Transition States − BS1. On the basis of the relative energies of the highest energy transition states in the GT pathway (**TS3**−**4**: −0.2 kcal/mol) and CH pathway (**TS6**−**7**: 6.5 kcal/mol) at the B3LYP/BS1 level of theory, we concluded in our previous communication that the GT mechanism is favored by over 6 kcal/mol with the model ligands that were employed.[10] However, the mechanisms for Si−C and C−H bond formation in two pathways are very distinct from each other; in the GT pathway, Si−C and C−H bond formation occurs via the insertion of ethylene into the Si−H bond at a location remote from the Ru atom, whereas, in the CH pathway, the Si−C and C−H bond formation occurs in the coordination sphere of the Ru center. In addition, the two highest energy transition states, **TS3**−**4** and **TS6**−**7**, are quite different; in the GT transition state (**TS3**−**4**), no new bonds are being formed to ruthenium, whereas, in the oxidative addition transition state (**TS6**−**7**), new Ru−H and Ru−Si bonds are formed. Thus, we sought to investigate if the

TABLE 4: Gas-Phase Relative Electronic Energies (kcal/mol) of the Key Intermediates and Transition State Structures Calculated Using Basis Sets 1−6 at B3LYP/BS1 Geometries with the Electronic Energy of 3 Set to 0.00 kcal/mol

		GT Pathway			CH Pathway			TS
method	basis set	**3**	**TS3−4**	**4**	**6**	**TS6−7**	7	diff.[a]
				DFT methods				
B3LYP	BS1	0.00	8.34	−29.50	−8.45	15.00	−3.84	6.66
	BS2	0.00	8.34	−30.08	−8.56	14.60	−3.65	6.26
	BS3	0.00	8.27	−28.12	−6.32	15.72	−2.71	7.45
	BS4	0.00	8.27	−28.28	−6.13	15.88	−2.44	7.61
	BS5	0.00	8.79	−26.47	−3.72	18.17	−0.60	9.38
	BS6	0.00	8.79	−27.00	−3.22	17.99	0.12	9.20
B3PW91	BS1	0.00	5.33	−29.78	−7.30	13.67	−5.38	8.34
	BS2	0.00	5.33	−30.35	−7.46	13.22	−5.26	7.89
OLYP	BS1	0.00	4.39	−28.83	−4.63	12.72	−3.05	8.33
	BS2	0.00	4.33	−29.48	−4.77	12.29	−2.92	7.96
O3LYP	BS1	0.00	3.33	−30.05	−6.44	11.82	−5.86	8.49
	BS2	0.00	3.32	−30.71	−6.58	11.36	−5.71	8.04
MPWPW91	BS1	0.00	3.84	−26.24	−6.15	10.45	−5.85	6.61
	BS2	0.00	3.82	−26.95	−6.46	9.93	−5.81	6.11
MPW1PW91	BS1	0.00	5.27	−30.62	−8.00	13.72	−6.10	8.45
	BS2	0.00	5.26	−31.26	−8.12	13.28	−5.96	8.02
PBEPBE	BS1	0.00	3.25	−26.26	−6.13	9.84	−6.50	6.59
	BS2	0.00	3.24	−27.00	−6.45	9.29	−6.47	6.05
PBE1PBE	BS1	0.00	4.73	−30.58	−7.92	13.20	−6.64	8.47
	BS2	0.00	4.73	−31.15	−8.05	12.73	−6.50	8.00
				WFT methods				
HF	BS1	0.00	16.71	−44.17	−16.82	32.22	0.45	15.51
	BS2	0.00	16.68	−44.40	−16.50	32.72	1.04	16.04
	BS3	0.00	16.55	−42.08	−13.89	33.58	1.90	17.03
	BS4	0.00	16.57	−42.07	−13.74	33.61	1.96	17.04
	BS5	0.00	17.50	−40.74	−11.29	36.57	4.34	19.07
	BS6	0.00	17.34	−41.04	−10.43	36.41	5.04	19.07
MP2	BS1	0.00	8.55	−16.46	−7.30	−7.99	−17.93	−16.54
	BS2	0.00	7.44	−15.04	−6.41	−10.19	−18.77	−17.63
	BS3	0.00	7.91	−12.56	−1.94	−6.27	−15.68	−14.19
	BS4	0.00	7.91	−12.18	−2.37	−6.41	−16.04	−14.33
	BS5	0.00	8.24	−11.14	0.40	−3.82	−13.57	−12.06
	BS6	0.00	6.88	−9.18	3.12	−4.39	−13.15	−11.27
MP3	BS1	0.00	11.28	−32.50	−12.38	22.54	−4.67	11.26
	BS2	0.00	11.06	−35.34	−13.18	24.77	−3.26	13.70
	BS3	0.00	11.43	−32.50	−10.06	25.75	−2.27	14.32
	BS4	0.00	11.30	−32.74	−10.27	26.45	−2.07	15.15
	BS5	0.00	11.92	−31.12	−7.75	28.92	0.06	17.00
	BS6	0.00	10.78	−30.38	−4.95	29.63	1.23	18.85
MP4SDQ	BS1	0.00	11.34	−22.77	−11.59	−5.44	−14.61	−16.78
	BS2	0.00	3.62	−21.50	−7.83	−1.63	−9.78	−5.26
	BS3	0.00	9.83	−21.50	−6.80	−1.05	−11.84	−10.88
	BS4	0.00	10.28	−21.55	−5.63	0.70	−10.03	−9.58
	BS5	0.00	10.22	−20.03	−4.44	1.60	−9.58	−8.62
	BS6	0.00	9.06	−19.30	−2.26	2.02	−8.66	−7.04
CISD	BS1	0.00	13.28	−37.12	−15.28	19.54	−6.07	6.26
	BS2	0.00	13.09	−38.37	−15.42	20.44	−5.47	7.35
	BS3	0.00	13.18	−35.43	−11.91	22.02	−4.02	8.84
	BS4	0.00	13.22	−35.73	−12.16	22.44	−3.97	9.22
	BS5	0.00	13.87	−34.14	−9.52	25.01	−1.66	11.14
CCSD	BS1	0.00	11.01	−29.73	−13.46	9.93	−9.41	−1.08
	BS2	0.00	10.41	−31.02	−13.24	11.53	−8.54	1.12
	BS3	0.00	10.69	−27.90	−9.54	13.50	−6.81	2.80
	BS4	0.00	10.62	−28.36	−9.81	14.14	−6.66	3.52
	BS5	0.00	11.12	−26.48	−7.21	16.44	−4.53	5.32
CCSD(T)	BS1	0.00	10.22	−27.21	−13.72	6.53	−11.34	−3.70
	BS2	0.00	9.03	−27.57	−13.18	6.77	−10.92	−2.27
	BS3	0.00	9.71	−24.93	−9.84	8.99	−9.30	−0.72
	BS4	0.00	9.63	−25.38	−10.11	9.63	−9.14	0.00
	BS5	0.00	10.04	−23.56	−7.53	11.87	−7.10	1.83

[a] TS diff. = [E(**TS6−7**) − E(**TS3−4**)] (kcal/mol).

conclusion that the GT mechanism is energetically favored was unduly influenced by the choice of B3LYP/BS1 as the level of theory.

For this investigation, the key steps in the GT and CH mechanisms, namely, ethylene insertion into the Si−H bond (**3** → **TS3−4** → **4**; Figure 1) and oxidation addition of the Si−H bond to Ru (**6** → **TS6−7** → **7**; Figure 2), respectively, were examined using a range of DFT and WFT methods. The relative energies of these structures were recalculated using the B3LYP/BS1 geometries and BS1 with the DFT methods B3PW91, MPWPW91, MPW1PW91, OLYP, O3LYP, PBEPBE, and PBE1PBE, and the WFT methods HF, MP2, MP3, MP4SDQ,

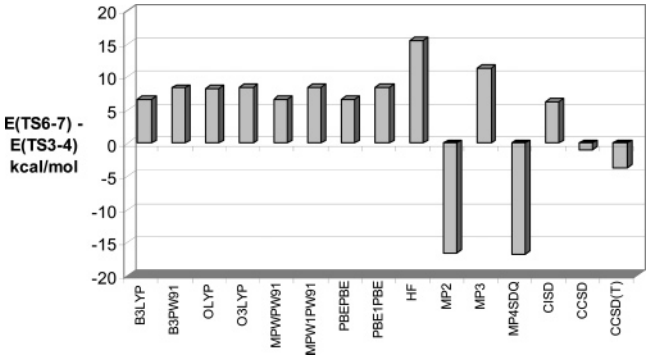

Figure 3. Energy differences [*E*(**TS6**−**7**) − *E*(**TS3**−**4**)] (kcal/mol) between key transition states in the GT and CH pathways, as calculated with various DFT and WFT methods and BS1.

CISD, CCSD, and CCSD(T). These calculations aimed to determine the influence of the theoretical method on the relative energies of the reaction intermediates and transition states (Table 3).

All of the DFT methods tested herein with BS1 calculated **TS3**−**4** to be lower in energy than **TS6**−**7**, with the difference in energy, [*E*(**TS6**−**7**) − *E*(**TS3**−**4**)], ranging from 6.6 to 8.5 kcal/mol (Table 3, Figure 3). Thus, all of the DFT/BS1 calculations predict that the GT mechanism is favored over the CH pathways that proceed through the oxidative addition transition state **TS6**−**7**. While all of the DFT methods tested herein calculated similar energy differences between **TS3**−**4** and **TS6**−**7** with BS1, the WFT methods produced a much larger range of energy differences [*E*(**TS6**−**7**) − *E*(**TS3**−**4**)] (Table 3, Figure 3). The HF/BS1 and MP3/BS1 levels of theory calculate the GT transition state **TS3**−**4** to be lower in energy than the CH transition state **TS6**−**7** by the largest amounts (15.5 and 11.3 kcal/mol, respectively), whereas the MP2/BS1 and MP4SDQ/BS1 levels of theory give the opposite results and calculate the CH transition state **TS6**−**7** to be lower in energy than the GT transition state **TS3**−**4** by over 16 kcal/mol. These values for [*E*(**TS6**−**7**) − *E*(**TS3**−**4**)] are indicative of oscillatory behavior in the Møller−Plesset perturbation series, which has been observed previously in other transition-metal systems.[12,50]

CISD, CCSD, and CCSD(T) are considered to be the higher accuracy WFT methods;[13,51] thus, these results are of significant interest. The CISD/BS1 level of theory calculates the GT transition state **TS3**−**4** to be 6.3 kcal/mol lower in energy than the CH transition state **TS6**−**7**, which is in good agreement with the DFT/BS1 calculations. In contrast, the CCSD/BS1 and CCSD(T)/BS1 levels of theory calculate the CH transition state **TS6**−**7** to be lower in energy than the GT transition state **TS3**−**4** by 1.1 and 3.7 kcal/mol, respectively. Thus, the CCSD/BS1 and CCSD(T)/BS1 calculations predict the CH mechanism to be favored, which directly contradicts all of the DFT/BS1 and CISD/BS1 calculations. Furthermore, CCSD(T)/BS1 calculates an energy difference [*E*(**TS6**−**7**) − *E*(**TS3**−**4**)] of −3.7 kcal/mol; this energy difference is more than 10 kcal/mol less than the difference calculated by all of the DFT methods, which is somewhat disconcerting because of the widespread use of DFT methods to study reaction mechanisms in transition-metal chemistry.

C. Single-Point Calculations with Larger Basis Sets. One possible cause of the discrepancy in the energy difference between **TS3**−**4** and **TS6**−**7** calculated at the CCSD(T)/BS1 and DFT/BS1 levels of theory is the choice of basis set. WFT methods that include electron correlation typically show larger basis set dependence than DFT methods.[13] Thus, to investigate the possibility that the discrepancies in [*E*(**TS6**−**7**) − *E*(**TS3**−**4**)] for the CCSD(T)/BS1 and DFT/BS1 calculations were due to basis set effects, the relative energies of **3**, **TS3**−**4**, **4**, **6**, **TS6**−**7**, and **7** were recalculated at the B3LYP/BS1 geometries using the B3LYP, HF, MP2, MP3, MP4SDQ, CISD, CCSD and CCSD(T) methods with five larger basis sets (BS2, BS3, BS4, BS5, and BS6). It should be noted that CISD, CCSD, and CCSD(T) calculations could not be completed with BS6 because of the large number of basis functions. However, HF, MP2, MP3 and MP4SDQ single-point energies for all structures were attained with BS6. The single-point energies were used to calculate the relative energies and [*E*(**TS6**−**7**) − *E*(**TS3**−**4**)] for all of the methods and basis sets. The relative energies of **3**, **TS3**−**4**, **4**, **6**, **TS6**−**7**, and **7** are provided in Table 4. Before discussing these results in detail, we will describe how we extrapolate these calculations to even larger basis sets.

D. Estimating the CISD, CCSD, and CCSD(T) BS6 Energies of TS3−**4 and TS6**−**7.** Because CISD, CCSD, and CCSD(T) calculations could not be completed with BS6 for **TS3**−**4** and **TS6**−**7**, we sought to estimate the BS6 CISD, CCSD, and CCSD(T) energies for **TS3**−**4** and **TS6**−**7** from the HF, MP2, MP3 and MP4SDQ energies calculated with basis sets 1−6 and the CISD, CCSD, and CCSD(T) energies calculated with basis sets 1−5.

A general practice in computational chemistry to estimate the energies of molecules at levels of theory that cannot be explicitly calculated (i.e., expensive methods with large basis sets) is to generate an estimate of the energy using a series of calculations at lower levels of theory (i.e., the Gaussian-*n* (G*n*) theories[52−55]). For example, the energy of a molecule at a given method (Method-A) and basis set (BS*x*) can be estimated from the energy calculated using a less expensive method (Method-B) with BS*x* and the difference in energies calculated using Method-A and Method-B with a smaller basis set (BS(*x*−1)) using eq 1:[56]

$$E^{\mathrm{BS}x}_{\mathrm{Method-A}}(\mathrm{est}) = E^{\mathrm{BS}x}_{\mathrm{Method-B}} + (E^{\mathrm{BS}(x-1)}_{\mathrm{Method-A}} - E^{\mathrm{BS}(x-1)}_{\mathrm{Method-B}}) \quad (1)$$

Note that, for WFT methods that include electron correlation, the WFT energies can be separated into Hartree−Fock (HF) and correlation energy terms using eq 2:[57]

$$E^{\mathrm{BS}x}_{\mathrm{Method}-i} = E^{\mathrm{BS}x}_{\mathrm{HF}} + E^{\mathrm{BS}x}_{\mathrm{corr}-i} \quad (2)$$

Thus, to estimate the BS6 CISD, CCSD, and CCSD(T) energies for **TS3**−**4** and **TS6**−**7**, only the BS6 CISD, CCSD, and CCSD(T) correlation energies need to be estimated, since the HF/BS6 energies were successfully calculated. To this end, eq 1 can be expressed in terms of the correlation energies obtained using Methods A and B and basis sets *x* and *x* − 1 as follows in eq 3:

$$E^{\mathrm{BS}x}_{\mathrm{Corr-A}}(\mathrm{est}) = E^{\mathrm{BS}x}_{\mathrm{Corr-B}} + (E^{\mathrm{BS}(x-1)}_{\mathrm{Corr-A}} - E^{\mathrm{BS}(x-1)}_{\mathrm{Corr-B}}) \quad (3)$$

Equation 3 estimates the Method-A/BS*x* correlation energy by assuming that the correlation energies from Methods A and B increase the same amount upon increasing the basis set size, and also that the difference in correlation energies from Methods A and B are the same for the two basis sets. From our calculations using basis sets 1−5, in which Method A is CISD, CCSD or CCSD(T) and Method B is MP2, MP3, or MP4SDQ, we observed that the difference in the correlation energies for the methods was not the same for all of the basis sets. Thus, eq 3 was modified to remove the assumption that the correlation energies from Methods A and B increase at the same rate by

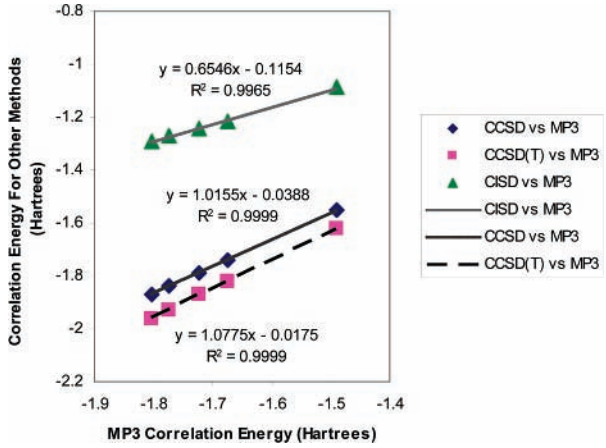

Figure 4. Plots of the CISD, CCSD, and CCSD(T) correlation energies vs the MP3 correlation energies for **TS3**−**4** for basis sets 1−5.

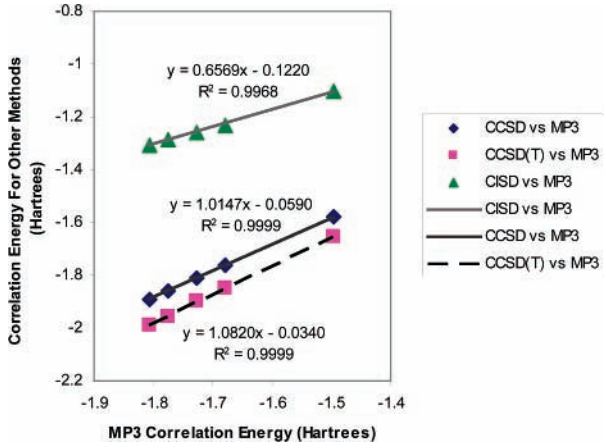

Figure 5. Plots of the CISD, CCSD, and CCSD(T) correlation energies vs the MP3 correlation energies for **TS6**−**7** for basis sets 1−5.

adding the coefficient m and replacing the term

$$(E_{\text{Corr-A}}^{\text{BS}(x-1)} - E_{\text{Corr-B}}^{\text{BS}(x-1)})$$

with the constant, b, to give eq 4:

$$E_{\text{Corr-A}}^{\text{BS}x}(\text{est}) = mE_{\text{Corr-B}}^{\text{BS}x} + b \tag{4}$$

in which the Corr-A term refers to the correlation energies from the CISD, CCSD, and CCSD(T) methods, the Corr-B term refers to the correlation energies from the MP2, MP3, and MP4SDQ methods, m and b are determined from a linear fit of the Method A and Method B correlation energies for basis sets 1−5, and the accuracy of the fit is judged by the R^2 value. Examination of the R^2 values of the linear fits revealed that the MP3 method provided the best R^2 values; thus, the basis set 6 correlation energies of **TS3**−**4** and **TS6**−**7** for the CISD, CCSD, and CCSD(T) were estimated using eq 5:

$$E_{\text{Corr-A}}^{\text{BS6}}(\text{est}) = mE_{\text{Corr-MP3}}^{\text{BS6}} + b \tag{5}$$

in which the Corr-A term refers to the BS6 correlation energies for the CISD, CCSD, and CCSD(T) methods, the Corr-MP3 term refers to the MP3/BS6 correlation energies, and m and b were obtained from linear fits of the basis set 1−5 data and are provided for the CISD, CCSD, and CCSD(T) methods for **TS3**−**4** and **TS6**−**7** in Figures 4 and 5, respectively. The BS6 CISD, CCSD, and CCSD(T) correlation energies for **TS3**−**4** and **TS6**−**7** that were estimated using eq 5 are provided in italics in Tables 5 and 6, respectively. Adding the BS6 CISD, CCSD, and CCSD(T) correlation energies to the HF/BS6 energies generates estimates of the CISD/BS6, CCSD/BS6, and CCSD(T)/BS6 energies for **TS3**−**4** and **TS6**−**7**, from which the energy differences between the transition states [E(**TS6**−**7**) − E(**TS3**−**4**)] for the CISD/BS6, CCSD/BS6, and CCSD(T)/BS6 levels of theory were estimated (see Table S1 (Supporting Information) and Figure 6).

E. Extrapolation to BS7. BS5 and BS6 both use the Stuttgart 1997 ECP basis set with added f-polarization functions on Ru. However, BS5 and BS6 use correlation-consistent double-ζ (cc-pVDZ) and triple-ζ (cc-pVTZ) basis sets on all other atoms; therefore, we sought to extrapolate the HF, MP2, MP3, MP4SDQ, CISD, CCSD, and CCSD(T) energies of **TS3**−**4** and **TS6**−**7** to the BS7 level, where BS7 is a hypothetical basis set that consists of the Stuttgart 1997 ECP basis set with added f-polarization functions on Ru and extrapolated basis sets on all other atoms. The WFT energies for **TS3**−**4** and **TS6**−**7** were extrapolated to BS7 using eqs 6, 7, and 8, which extrapolate the HF energy (eq 7)[58] and the correlation energy (eq 8)[59] separately,[57] while the B3LYP energy was extrapolated using eq 8:

$$E_{\text{Method}}^{\text{BS7}} = E_{\text{HF}}^{\text{BS7}} + E_{\text{corr,method}}^{\text{BS7}} \tag{6}$$

$$E_{\text{HF}}^{\text{BS7}} = \frac{x^5 E_{\text{HF}}^{\text{BS5}} - y^5 E_{\text{HF}}^{\text{BS6}}}{x^5 - y^5} \tag{7}$$

$$E_{\text{corr,method}}^{\text{BS7}} = \frac{x^3 E_{\text{corr,method}}^{\text{BS5}} - y^3 E_{\text{coor,method}}^{\text{BS6}}}{x^3 - y^3} \tag{8}$$

in which $x = 2$ for BS5 and $y = 3$ for BS6, since BS5 and BS6 use cc-pVDZ and cc-pVTZ basis sets, respectively, for Si, P, C, and H.

The extrapolated correlation and HF energies for **TS3**−**4** and **TS6**−**7** are presented in italics in Tables 5 and 6, respectively. The extrapolated BS7 B3LYP and WFT energies for **TS3**−**4** and **TS6**−**7** were used to estimate the energy difference between these transitions states [E(**TS6**−**7**) − E(**TS3**−**4**)]. The values for [E(**TS6**−**7**) − E(**TS3**−**4**)] are presented in Table S1 and Figure 6. These extrapolated BS7 results[61] serve as the best estimates for [E(**TS6**−**7**) − E(**TS3**−**4**)] as calculated by the various WFT methods.

F. Summary of Basis Set Effects on the Difference in Energy between TS3−**4 and TS6**−**7.** The energy differences [E(**TS6**−**7**) − E(**TS3**−**4**)] between the CH transition state **TS6**−**7** and the GT transition state **TS3**−**4**, as calculated using a range of theoretical methods and basis sets, are presented in Table S1 (Supporting Information) and Figure 6. The difference in energy between the CH transition state and the GT transition state [E(**TS6**−**7**) − E(**TS3**−**4**)] is highly dependent on the theoretical method. For all basis sets tested herein, the B3LYP, HF, MP3, and CISD methods calculated the energy of **TS3**−**4** to be lower than the energy of **TS6**−**7**, which is indicated by the positive value for [E(**TS6**−**7**) − E(**TS3**−**4**)]. In contrast, for all basis sets, MP2 and MP4SDQ calculated negative values for [E(**TS6**−**7**) − E(**TS3**−**4**)]. For CCSD, all basis sets except BS1 yielded positive values for [E(**TS6**−**7**) − E(**TS3**−**4**)]. For CCSD(T), basis sets 1−3 yielded negative values for [E(**TS6**−**7**) − E(**TS3**−**4**)], basis set 4 yielded equal energies for **TS3**−**4** and **TS6**−**7**, and basis sets 5−7 predicted positive values for [E(**TS6**−**7**) − E(**TS3**−**4**)].

For all methods, the energy difference [E(**TS6**−**7**) − E(**TS3**−**4**)] depends on the basis set, with the smallest basis set

TABLE 5: HF Electronic Energies (hartrees) and MP2, MP3, MP4SDQ, CISD, CCSD, and CCSD(T) Correlation Energies (hartrees) for TS3−4 for Basis Sets 1−7[a]

		correlation energies					
	HF energy	MP2	MP3	MP4SDQ	CISD	CCSD	CCSD(T)
BS1	−377.294278	−1.476782	−1.489083	−1.579969	−1.086884	−1.550915	−1.622135
BS2	−377.321734	−1.813086	−1.802138	−1.919648	−1.292510	−1.868566	−1.959885
BS3	−378.306166	−1.723067	−1.673734	−1.771394	−1.218861	−1.739110	−1.821972
BS4	−378.323714	−1.786653	−1.773104	−1.877052	−1.272725	−1.840384	−1.928686
BS5	−997.879021	−1.767119	−1.722673	−1.820118	−1.244178	−1.786619	−1.871510
BS6	−997.988797	−2.072386	−2.006771	−2.099109	*−1.428985*	*−2.076609*	*−2.179860*
BS7	*−998.005446*	*−2.200919*	*−2.126391*	*−2.216579*	*−1.506798*	*−2.198710*	*−2.309691*

[a] Values in italics were extrapolated as described in the text in Results and Discussion sections D and E.

TABLE 6: HF Electronic Energies (hartrees) and MP2, MP3, MP4SDQ, CISD, CCSD, and CCSD(T) Correlation Energies (hartrees) for TS6−7 for Basis Sets 1−7[a]

		correlation energies					
	HF energy	MP2	MP3	MP4SDQ	CISD	CCSD	CCSD(T)
BS1	−377.269555	−1.527859	−1.495862	−1.631426	−1.101633	−1.577365	−1.652749
BS2	−377.296169	−1.866751	−1.805868	−1.953591	−1.306363	−1.892352	−1.989061
BS3	−378.279031	−1.772808	−1.678047	−1.815863	−1.231914	−1.761779	−1.850259
BS4	−378.296556	−1.836643	−1.776113	−1.919470	−1.285196	−1.861936	−1.955845
BS5	−997.848635	−1.816724	−1.725969	−1.864246	−1.256818	−1.808525	−1.898987
BS6	−997.958403	−2.120743	−2.007121	−2.140718	*−1.440522*	*−2.095717*	*−2.205600*
BS7	*−997.975050*	*−2.248751*	*−2.125500*	*−2.257127*	*−1.517872*	*−2.216640*	*−2.334701*

[a] Values in italics were extrapolated as described in the text in Results and Discussion sections D and E.

dependence observed for the B3LYP and HF methods. Examination of the basis sets reveals specific components responsible for changing the relative energies of **TS3−4** and **TS6−7** for all theoretical methods. For example, BS1 and BS3 only differ in the basis functions for Ru, with all other atoms represented by the same basis functions. For all methods, [*E*(**TS6−7**) − *E*(**TS3−4**)] is more positive for BS3 than for BS1, indicating that the Stuttgart 1997 RSC + f basis set on Ru lowers the energy of **TS3−4** relative to that of **TS6−7**. BS3 and BS4 have the same basis functions for Ru, P, and Si; however, BS4 uses diffuse and polarization functions on all C and H, whereas BS3 uses polarization functions on all C and select H, but does not use diffuse functions on C or H atoms. Comparing the B3LYP, HF, and MP2 results of [*E*(**TS6−7**) − *E*(**TS3−4**)] for BS3 and BS4 reveals changes of less than 0.2 kcal/mol, whereas, for MP3, MP4SDQ, CISD, CCSD, and CCSD(T) for BS3 and BS4 in all cases, [*E*(**TS6−7**) − *E*(**TS3−4**)] is more positive for BS4, albeit by small amounts (0.4 to 1.3 kcal/mol). BS4 and BS5 use the same basis functions for Ru; however, BS4 uses LANL2DZdp basis sets for Si and P and 6-31++G(d′,p′) basis sets for C and H, whereas BS5 uses cc-pVDZ basis sets for Si, P, C, and H. For all methods, [*E*(**TS6−7**) − *E*(**TS3−4**)] is more positive for BS5 relative to BS4. BS5 and BS6 also use the same basis functions for Ru; however, BS5 uses cc-pVDZ basis functions for Si, P, C, and H, whereas BS6 uses cc-pVTZ basis functions for Si, P, C, and H. For HF, [*E*(**TS6−7**) − *E*(**TS3−4**)] does not change between BS5 and BS6; however, for MP2, MP3, MP4SDQ, CISD, CCSD, and CCSD(T), [*E*(**TS6−7**) − *E*(**TS3−4**)] is more positive for BS6 than for BS5. The BS5 and BS6 results indicate that, as additional basis functions are added to represent the atoms, [*E*(**TS6−7**) − *E*(**TS3−4**)] becomes more positive for the WFT methods other than HF, which must be due to basis set effects on correlation energy because [*E*(**TS6−7**) − *E*(**TS3−4**)] is essentially equivalent at the HF/BS5 and HF/BS6 levels of theory.

Extrapolation of the MP2, MP3, MP4SDQ, CISD, CCSD, and CCSD(T) energies of **TS3−4** and **TS6−7** to BS7 from the BS5 and BS6 results suggest that [*E*(**TS6−7**) − *E*(**TS3−4**)] will continue to become more positive for these WFT methods as the number of basis functions on the Si, P, C, and H increase.

G. Effects of Basis Sets and Methods on Barrier Heights. Because the energies of structures **3**, **TS3−4**, **4**, **6**, **TS6−7**,

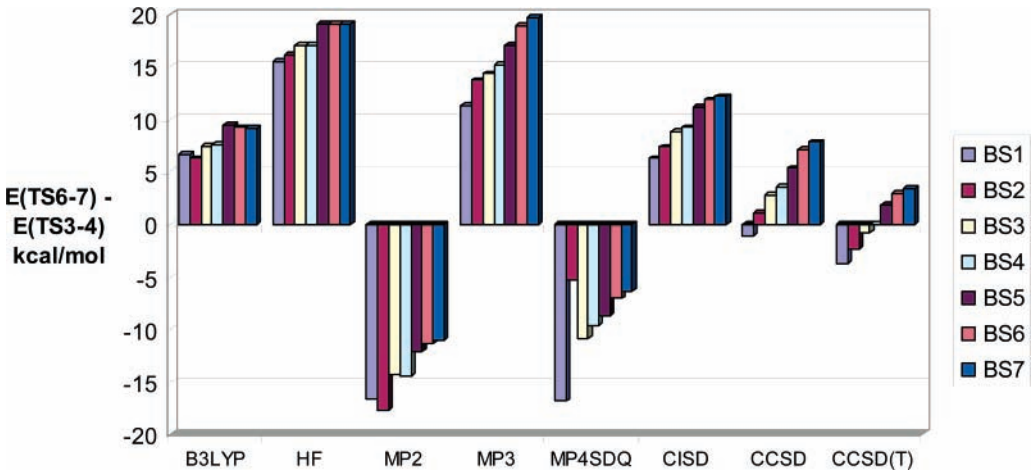

Figure 6. Energy differences between **TS3−4** and **TS6−7** [*E*(**TS6−7**) − *E*(**TS3−4**)] (kcal/mol) for various basis sets and theoretical methods.

TABLE 7: Electronic Energy Barriers (kcal/mol) of the Forward and Reverse Steps 3 → TS3−4, 4 → TS3−4, 6 → TS6−7, and 7 → TS6−7, Calculated with Various DFT and WFT Methods for Basis Sets 1−6

method	basis set	GT pathway		CH pathway	
		3 → TS3−4	**4 → TS3−4**	**6 → TS6−7**	**7 → TS6−7**
		DFT methods			
B3LYP	BS1	8.34	37.84	23.45	18.84
	BS2	8.34	38.42	23.16	18.25
	BS3	8.27	36.39	22.04	18.43
	BS4	8.27	36.55	22.01	18.32
	BS5	8.79	35.26	21.89	18.77
	BS6	8.79	35.79	21.21	17.87
B3PW91	BS1	5.33	35.11	20.97	19.05
	BS2	5.33	35.68	20.68	18.48
OLYP	BS1	4.39	33.22	17.35	15.77
	BS2	4.33	33.81	17.06	15.21
O3LYP	BS1	3.33	33.38	18.26	17.68
	BS2	3.32	34.03	17.94	17.07
MPWPW91	BS1	3.84	30.08	16.60	16.30
	BS2	3.82	30.77	16.39	15.74
MPW1PW91	BS1	5.27	35.89	21.72	19.82
	BS2	5.26	36.52	21.40	19.24
PBEPBE	BS1	3.25	29.51	15.97	16.34
	BS2	3.24	30.24	15.74	15.76
PBE1PBE	BS1	4.73	35.31	21.12	19.84
	BS2	4.73	35.88	20.78	19.23
		WFT methods			
HF	BS1	16.71	60.88	49.04	31.77
	BS2	16.68	61.08	49.22	31.68
	BS3	16.55	58.63	47.47	31.68
	BS4	16.57	58.64	47.35	31.65
	BS5	17.50	58.24	47.86	32.23
	BS6	17.34	58.38	46.84	31.37
MP2	BS1	8.55	25.01	−0.69	9.94
	BS2	7.44	22.48	−3.78	8.58
	BS3	7.91	20.47	−4.33	9.41
	BS4	7.91	20.09	−4.04	9.63
	BS5	8.24	19.38	−4.22	9.75
	BS6	6.88	16.06	−7.51	8.76
MP3	BS1	11.28	43.78	34.92	27.21
	BS2	11.06	46.40	37.95	28.03
	BS3	11.43	43.93	35.81	28.02
	BS4	11.30	44.04	36.72	28.52
	BS5	11.92	43.04	36.67	28.86
	BS6	10.78	41.16	34.58	28.40
MP4SDQ	BS1	11.34	34.11	6.15	9.17
	BS2	3.62	25.12	6.20	8.15
	BS3	9.83	31.33	5.75	10.79
	BS4	10.28	31.83	6.33	10.73
	BS5	10.22	30.25	6.04	11.18
	BS6	9.06	28.36	4.28	10.68
CISD	BS1	13.28	50.40	34.82	25.61
	BS2	13.09	51.46	35.86	25.91
	BS3	13.18	48.61	33.93	26.04
	BS4	13.22	48.95	34.60	26.41
	BS5	13.87	48.01	34.53	26.67
CCSD	BS1	11.01	40.74	23.39	19.34
	BS2	10.41	41.43	24.77	20.07
	BS3	10.69	38.59	23.04	20.31
	BS4	10.62	38.98	23.95	20.80
	BS5	11.12	37.60	23.65	20.97
CCSD(T)	BS1	10.22	37.43	20.25	17.87
	BS2	9.03	36.60	19.95	17.69
	BS3	9.71	34.64	18.83	18.29
	BS4	9.63	35.01	19.74	18.77
	BS5	10.04	33.60	19.40	18.97

and **7** were calculated using a range of methods and basis sets, the effects of the computational methodology on the two forward and two reverse energetic barriers, namely, **3 → TS3−4**, **4 → TS3−4**, **6 → TS6−7**, and **7 → TS6−7**, can be examined. The energetic barriers for these four steps calculated with the DFT and WFT methods with basis sets 1−6 are presented in Table 7.

For the barrier heights from the DFT methods, results from calculations using BS1 and BS2 reveal that the B3LYP method calculates the highest barriers for **3 → TS3−4**, **4 → TS3−4**, and **6 → TS6−7**, whereas PBE1PBE and MPW1PW91 calculate the highest barriers for **7 → TS6−7**. In general, the DFT methods that do not incorporate HF exchange, namely, OLYP, MPWPW91, and PBEPBE, calculated the lowest barriers for these four transitions.

TABLE 8: T1 Diagnostic Values for Structures 3, TS3−4, 4, 6, TS6−7, and 7 for Basis Sets 1−5

basis set	GT pathway			CH pathway		
	3	**TS3−4**	**4**	**6**	**TS6−7**	**7**
BS1	0.0193	0.0201	0.0224	0.0230	0.0204	0.0196
BS2	0.0184	0.0194	0.0216	0.0219	0.0191	0.0185
BS3	0.0191	0.0200	0.0223	0.0226	0.0196	0.0191
BS4	0.0189	0.0198	0.0222	0.0225	0.0195	0.0190
BS5	0.0189	0.0199	0.0223	0.0225	0.0195	0.0190

For the barrier heights from the WFT methods, results from calculations using basis sets 1−6 for HF, MP2, MP3, and MP4SDQ, and basis sets 1−5 for CISD, CCSD, and CCSD(T) indicate that the HF and MP2 methods calculate the highest and lowest barriers, respectively, for all of the transitions. Large discrepancies between HF and MP2 barriers and oscillations in the energies of the MP*x* series are often indicative of the multireference character of the intermediates or transition states. To examine this issue, the T1 diagnostic values[60] of the species involved were calculated. The results presented in Table 8 indicate that structures **4** and **6** have more multireference character than the corresponding transition states, as indicated by the higher T1 values. Also of interest is that, in the GT pathway, the multireference character increases as the reaction proceeds in the forward direction from **3 → TS3−4 → 4**, whereas in the CH pathway, the multireference character decreases as the reaction proceeds in the forward direction from **6 → TS6−7 → 7**. These changes in multireference character cause large oscillations in the MP*x* series for the barrier of the reverse reaction in the GT pathway, **4 → TS3−4**, and for the barrier of the forward reaction in the CH pathway, **6 → TS6−7**. In addition, the changes in multireference character cause large oscillations in the MP*x* series for the exothermicities of the forward reactions in the two pathways (i.e., **3 → 4** and **6 → 7**). However, also of interest is that the T1 calculations indicate that the two transition states, **TS3−4** and **TS6−7**, have similar multireference character.

It is also informative to compare the B3LYP DFT and WFT results for the barrier heights. For the basis sets tested herein, the HF, MP3, and CISD methods calculate significantly higher barriers than does the B3LYP DFT method for all four transitions, with the MP3 and CISD methods giving better agreement with the B3LYP values. For all basis sets, MP2 and MP4SDQ calculate lower barriers than does B3LYP for **4 → TS3−4**, **6 → TS6−7**, and **7 → TS6−7**, with the MP4SDQ barriers typically being closer to the B3LYP barriers. For **3 → TS3−4**, the barriers calculated using basis sets 1−6 and B3LYP, MP2, and MP4SDQ are similar.

The CCSD method generally calculated slightly higher barriers than the B3LYP method for all transitions, with the largest difference in barrier height being only 3.01 kcal/mol. For **3 → TS3−4**, CCSD(T) calculated slightly higher barriers than did B3LYP for basis sets 1−5. In contrast, however, for **4 → TS3−4** and **6 → TS6−7**, CCSD(T) calculated slightly lower barriers than did B3LYP for basis set 1−5, with the largest differences observed for **6 → TS6−7** (−3.21 kcal/mol with basis sets 2 and 3). For **7 → TS6−7**, the CCSD(T) and B3LYP barriers were within 1 kcal/mol for basis sets 1−5.

In terms of the basis set dependence of the methods, examination of the results from basis sets 1−5, which allows

B3LYP to be compared to the WFT results, suggests that the Møller−Plesset methods, in particular MP2 and MP4SDQ, display higher basis set dependence than do the other methods, as indicated by larger ranges of barrier heights for basis sets 1−5. In contrast, the B3LYP and HF methods generally displayed the smallest ranges of barrier heights for basis sets 1−5, whereas CISD, CCSD, and CCSD(T) displayed ranges larger than the B3LYP methods for the four barriers with basis sets 1−5.

IV. Conclusions

We have conducted an extensive evaluation of the influence of computational methodology on the relative energies of key intermediates and transition states in two potential hydrosilylation mechanisms. All of the DFT methods tested herein calculated the transition state from the GT mechanism (**TS3**−**4**) to be lower in energy than the transition state of the CH mechanism (**TS6**−**7**) by 6.5 to 8.5 kcal/mol. Similarly, the HF, MP3, and CISD WFT methods calculated the transition state from the GT mechanism (**TS3**−**4**) to be lower in energy than the transition state from the CH mechanism (**TS6**−**7**) for all of the basis sets used herein. In contrast, the MP2 and MP4SDQ WFT methods predicted the transition state from the CH mechanism (**TS6**−**7**) to be lower in energy than **TS3**−**4** for all of the basis sets we tested. For all basis sets, except the smallest basis set (BS1), the CCSD WFT method calculated **TS3**−**4** to be lower in energy than **TS6**−**7**. Finally, the extrapolated basis set results indicated that the CCSD(T) method also predicts **TS3**−**4** to be lower in energy than **TS6**−**7** for large basis sets. These results suggest that initial discrepancies between DFT and CCSD(T) results observed for these transition-metal-catalyzed hydrosilylation pathways can arise because of basis set effects. Furthermore, these series of calculations suggest that large basis sets are required for CCSD(T) calculations on transition-metal systems, which limits the size of the systems that can be efficiently examined using CCSD(T) calculations, but that extrapolation techniques can be used effectively to extend the range of basis sets.

Acknowledgment. We thank the NSF (CHE 05-00184, DMS 02-16275) and the Welch Foundation (A-0648) for support.

Supporting Information Available: Table of data used to create Figure 6. Relative free energy profiles of the GT and CH pathways. Plots of the CISD, CCSD, and CCSD(T) correlation energies versus the MP2 and MP4SDQ correlation energies for **TS3**−**4** and **TS6**−**7** for basis sets 1−5. This material is available free of charge via the Internet at http://pubs.acs.org.

References and Notes

(1) Tilley, T. D. In *The Chemistry of Organic Silicon Compounds*; Patai, S., Rappoport, Z., Eds.; John Wiley & Sons Ltd.: New York, 1989; pp 1415−1477.

(2) Ojima, I. In *The Chemistry of Organic Silicon Compounds*; Patai, S., Rappoport, Z., Eds.; John Wiley & Sons Ltd.: New York, 1989; pp 1479−1526.

(3) Marciniec. B. *Appl. Organomet. Chem.* **2000**, *14*, 527−538.

(4) Marciniec, B. *Silicon Chem.* **2002**, *1*, 155−175.

(5) Carpentier, J.-F.; Bette, V. *Curr. Org. Chem.* **2002**, *6*, 913−936.

(6) Glaser, P. B.; Tilley, T. D. *J. Am. Chem. Soc.* **2003**, *125*, 13640−13641.

(7) For example, in the Chalk−Harrod mechanism, olefin inserts into the metal−hydrogen bond ((a) Chalk, A. J.; Harrod, J. F. *J. Am. Chem. Soc.* **1965**, *87*, 16−21. (b) Chalk, A. J.; Harrod, J. F. *J. Am. Chem. Soc.* **1965**, *87*, 1133−1135.), whereas, in the modified Chalk−Harrod mechanism proposed by Sietz and Wrighton, olefin inserts into the metal−silicon bond ((c) Seitz, F.; Wrighton, M. S. *Angew. Chem., Int. Ed. Engl.* **1988**, *27*, 289−291. (d) Duckett, S. B.; Perutz, R. N. *Organometallics* **1992**, *11*, 90−98.). Furthermore, σ-bond metathesis hydrosilylation mechanisms that are proposed for d^0 metals also occur within the first coordination sphere of the transition metal ((e) Corey, J. Y.; Zhu, X.-H. *Organometallics* **1992**, *11*, 672−683. (f) Kesti, M. R.; Waymouth, R. M. *Organometallics* **1992**, *11*, 1095−1103.).

(8) For theoretical investigations on other hydrosilylation catalysts, see (a) Sakaki, S.; Takayama, T.; Sumimoto, M.; Sugimoto, M. *J. Am. Chem. Soc.* **2004**, *126*, 3332−3348. (b) Chung, L. A.; Wu, Y.; Trost, B. M.; Ball, Z. T. *J. Am. Chem. Soc.* **2003**, *125*, 11578−11582. (c) Sakaki, S.; Sumimoto, M.; Fukuhara, M.; Sugimoto, M.; Fujimoto, H.; Matsuzaki, S. *Organometallics* **2002**, *21*, 3788−3802 and references therein.

(9) Brunner, H. *Angew. Chem., Int. Ed.* **2004**, *43*, 2749−2750.

(10) Beddie, C.; Hall, M. B. *J. Am. Chem. Soc.* **2004**, *126*, 13564−13565.

(11) Fan, Y.; Hall, M. B. *Chem.—Eur. J.* **2004**, *10*, 1805−1814.

(12) Hall, M. B.; Fan, H.-J. *Adv. Inorg. Chem.* **2003**, *54*, 321−349.

(13) Niu, S.; Hall, M. B. *Chem. Rev.* **2000**, *100*, 353−405.

(14) (a) Cizek, J. *Adv. Chem. Phys.* **1969**, *14*, 35−89. (b) Purvis, G. D.; Bartlett, R. J. *J. Chem. Phys.* **1982**, *76*, 1910−1918. (c) Scuseria, G. E. Janssen, C. L.; Schaefer, H. F., III *J. Chem. Phys.* **1988**, *89*, 7382−7387. (d) Scuseria, G. E.; Schaefer, H. F., III *J. Chem. Phys.* **1989**, *90*, 3700−3703.

(15) (a) Raghavachari, K.; Trucks, G. W.; Pople, J. A.; Head-Gordon, M. *Chem. Phys. Lett.* **1989**, *157*, 479−483. (b) Pople, J. A.; Gordon-Head, M.; Raghavachari, K. *J. Chem. Phys.* **1987**, *87*, 5968−5975. (c) Watts, J. D.; Gauss, J.; Barlett, R. J. *J. Chem. Phys.* **1998**, *98*, 8718−8733.

(16) Preliminary results were initially reported as Beddie, C.; Hall, M. B. *Abstracts of Papers*, 229th ACS National Meeting, San Diego, CA, March 13−17, 2005; American Chemical Society: Washington, DC, 2005.

(17) All calculations were conducted using the Gaussian03 suite of programs: Frisch, M. J.; Trucks, G. W.; Schlegel, H. B.; Scuseria, G. E.; Robb, M. A.; Cheeseman, J. R.; Montgomery, J. A., Jr.; Vreven, T.; Kudin, K. N.; Burant, J. C.; Millam, J. M.; Iyengar, S. S.; Tomasi, J.; Barone, V.; Mennucci, B.; Cossi, M.; Scalmani, G.; Rega, N.; Petersson, G. A.; Nakatsuji, H.; Hada, M.; Ehara, M.; Toyota, K.; Fukuda, R.; Hasegawa, J.; Ishida, M.; Nakajima, T.; Honda, Y.; Kitao, O.; Nakai, H.; Klene, M.; Li, X.; Knox, J. E.; Hratchian, H. P.; Cross, J. B.; Adamo, C.; Jaramillo, J.; Gomperts, R.; Stratmann, R. E.; Yazyev, O.; Austin, A. J.; Cammi, R.; Pomelli, C.; Ochterski, J. W.; Ayala, P. Y.; Morokuma, K.; Voth, G. A.; Salvador, P.; Dannenberg, J. J.; Zakrzewski, V. G.; Dapprich, S.; Daniels, A. D.; Strain, M. C.; Farkas, O.; Malick, D. K.; Rabuck, A. D.; Raghavachari, K.; Foresman, J. B.; Ortiz, J. V.; Cui, Q.; Baboul, A. G.; Clifford, S.; Cioslowski, J.; Stefanov, B. B.; Liu, G.; Liashenko, A.; Piskorz, P.; Komaromi, I.; Martin, R. L.; Fox, D. J.; Keith, T.; Al-Laham, M. A.; Peng, C. Y.; Nanayakkara, A.; Challacombe, M.; Gill, P. M. W.; Johnson, B.; Chen, W.; Wong, M. W.; Gonzalez, C.; Pople, J. A. *Gaussian03*, revision B.4; Gaussian, Inc.: Pittsburgh, PA, 2003.

(18) Becke, A. D. *J. Chem. Phys.* **1993**, *98*, 5648−5652.

(19) Lee, C.; Yang, W.; Parr, R. G. *Phys. Rev. B* **1988**, *37*, 785−789.

(20) Couty, M.; Hall, M. B. *J. Comput. Chem.* **1996**, *17*, 1359−1370.

(21) (a) Hay, P. J.; Wadt, W. R. *J. Chem. Phys.* **1985**, *82*, 270−283. (b) Wadt, W. R.; Hay, P. J. *J. Chem. Phys.* **1985**, *82*, 284−298. (c) Hay, P. J.; Wadt, W. R. *J. Chem. Phys.* **1985**, *82*, 299−310.

(22) Ehlers, A. W.; Böhme, M.; Dapprich, S.; Gobbi, A.; Höllwarth, A.; Jonas, V.; Köhler, K. F.; Stegmann, R.; Veldkamp, A.; Frenking, G. *Chem. Phys. Lett.* **1993**, *208*, 111−114.

(23) Andrae, D.; Haeussermann, U.; Dolg, M.; Stoll, H.; Preuss, H. *Theor. Chim. Acta* **1990**, *77*, 123−141.

(24) Basis sets were obtained from the Extensible Computational Chemistry Environment Basis Set Database, version 02/25/04, as developed and distributed by the Molecular Science Computing Facility, Environmental and Molecular Sciences Laboratory, which is part of the Pacific Northwest Laboratory, P.O. Box 999, Richland, WA 99352, USA, and funded by the U.S. Department of Energy. The Pacific Northwest Laboratory is a multiprogram laboratory operated by Battelle Memorial Institute for the U.S. Department of Energy under contract DE-AC06−76RLO 1830. Contact Karen Schuchardt for further information.

(25) Check, C. E.; Faust, T. O.; Bailey, J. M.; Wright, B. J.; Gilbert, T. M.; Sunderlin, L. S. *J. Phys. Chem. A* **2001**, *105*, 8111−8116.

(26) Woon, D. E.; Dunning, T. H., Jr. *J. Chem. Phys.* **1993**, *98*, 1358−1371.

(27) Dunning, T. H., Jr. *J. Chem. Phys.* **1989**, *90*, 1007−1023.

(28) Ditchfield, R.; Hehre, W. J.; Pople, J. A. *J. Chem. Phys.* **1971**, *54*, 724−728.

(29) Hehre, W. J.; Ditchfield, R.; Pople, J. A. *J. Chem. Phys.* **1972**, *56*, 2257−2261.

(30) Hariharan, P. C.; Pople, J. A. *Theor. Chim. Acta* **1973**, *28*, 213−222.

(31) Petersson, G. A.; Al-Laham, M. A. *J. Chem. Phys.* **1991**, *94*, 6081−6090.

(32) Petersson, G. A.; Bennett, A.; Tensfeldt, T. G.; Al-Laham, M. A.; Shirley, W. A.; Mantzaris, J. *J. Chem. Phys.* **1988**, *89*, 2193−2218.

(33) Foresman, J. B.; Frisch, Æ. *Exploring Chemistry with Electronic Structure Methods*, 2nd ed.; Gaussian, Inc.: Pittsburgh, PA, 1996; p 110. The 6-31G(d′) basis set has the d polarization functions for C, N, O, and F taken from the 6-311G basis set, instead of the original arbitrarily assigned value of 0.8 used in the 6-31G(d) basis set.

(34) Clark, T.; Chandrasekhar, J.; Spitznagel, G. W.; Schleyer, P. v. R. *J. Comput. Chem.* **1983**, *4*, 294−301.

(35) (a) Burke, K.; Perdew, J. P.; Wang, Y. In *Electronic Density Functional Theory: Recent Progress and New Directions*; Dobson, J. F., Vignale, G., Das, M. P., Eds.; Plenum: New York, 1998; pp 81−111. (b) Perdew, J. P. In *Electronic Structure of Solids '91*; Ziesche, P., Eschrig, H., Eds.; Akademie Verlag: Berlin, 1991; p 11. (c) Perdew, J. P.; Chevary, J. A.; Vosko, S. H.; Jackson, K. A.; Pederson, M. R.; Singh, D. J.; Fiolhais, C. *Phys. Rev. B* **1992**, *46*, 6671−6687. (d) Perdew, J. P.; Chevary, J. A.; Vosko, S. H.; Jackson, K. A.; Pederson, M. R.; Singh, D. J.; Fiolhais, C. *Phys. Rev. B* **1993**, *48*, 4978. (e) Perdew, J. P.; Burke, K.; Wang, Y. *Phys. Rev. B* **1996**, *54*, 16533−16539.

(36) Adamo, C.; Barone, V. *J. Chem. Phys.* **1998**, *108*, 664−675.

(37) Handy, N. C.; Cohen, A. J. *Mol. Phys.* **2001**, *99*, 403−412.

(38) Cohen, A. J.; Handy, N. C. *Mol. Phys.* **2001**, *99*, 607−615.

(39) (a) Perdew, J. P.; Burke, K.; Ernzerhof, M. *Phys. Rev. Lett.* **1996**, *77*, 3865−3868. (b) Perdew, J. P.; Burke, K.; Ernzerhof, M. *Phys. Rev. Lett.* **1997**, *78*, 1396.

(40) (a) Roothan, C. C. J. *Rev. Mod. Phys.* **1951**, *23*, 69−89. (b) Pople, J. A. *J. Chem. Phys.* **1954**, *22*, 571−572. (c) McWeeny, R.; Diercksen, G. *J. Chem. Phys.* **1968**, *49*, 4852−4856.

(41) Moller, C.; Plessett, M. S. *Phys. Rev.* **1934**, *46*, 618−622.

(42) (a) Head-Gordon, M.; Pople, J. A.; Frisch, M. J. *Chem. Phys. Lett.* **1988**, *153*, 503−506. (b) Frisch, M. J.; Head-Gordon, M.; Pople, J. A. *Chem. Phys. Lett.* **1990**, *166*, 275−280. (c) Frisch, M. J.; Head-Gordon, M.; Pople, J. A. *Chem. Phys. Lett.* **1990**, *166*, 281−289. (d) Head-Gordon, M.; Head-Gordon, T. *Chem. Phys. Lett.* **1994**, *220*, 122−128. (e) Saebo, S.; Almlof, J. *Chem. Phys. Lett.* **1989**, *154*, 83−89.

(43) Pople, J. A.; Binkley, J. S.; Seeger, R. *Int. J. Quantum Chem. Symp.* **1976**, *10*, 1−19.

(44) Pople, J. A.; Seeger, R.; Krishnan, R. *Int. J. Quantum Chem. Symp.* **1977**, *11*, 149−163.

(45) Krishnan, R.; Pople, J. A. *Int. J. Quantum Chem.* **1978**, *14*, 91−100.

(46) (a) Krishnan, R.; Schlegel, H. B.; Pople, J. A. *J. Chem. Phys.* **1980**, *72*, 4654−4655. (b) Raghavachari, K.; Pople, J. A. *Int. J. Quantum Chem.* **1981**, *20*, 1067−1071.

(47) Manson, J.; Webster, C. E.; Hall, M. B. *JIMP Development*, version 0.1 (built for Windows PC and Redhat Linux 7.3); Department of Chemistry, Texas A&M University: College Station, TX, 2004. http://www.chem.tamu.edu/jimp/.

(48) Simon, S.; Duran, M.; Dannenberg, J. J. *J. Chem. Phys.* **1996**, *105*, 11024−11031.

(49) Boys, S. F.; Bernardi, F. *Mol. Phys.* **1970**, *19*, 553−566.

(50) Hyla-Kryspin, I.; Grimme, S. *Organometallics*, **2004**, *23*, 5581−5592.

(51) Torrent, M.; Solà, M.; Frenking, G. *Chem. Rev.* **2000**, *100*, 439−493.

(52) Pople, J. A.; Head-Gordon, M.; Fox, D. J.; Raghavachari, K.; Curtiss, L. A. *J. Chem. Phys.* **1989**, *90*, 5622−5629.

(53) Curtiss, L. A.; Jones, C.; Trucks, G. W.; Raghavachari, K.; Pople, J. A. *J. Chem. Phys.* **1990**, *93*, 2537−2545.

(54) Curtiss, L. A.; Raghavachari, K.; Trucks, G. W.; Pople, J. A. *J. Chem. Phys.* **1991**, *94*, 7221−7230.

(55) Curtiss, L. A.; Raghavachari, K.; Redfern, P. C.; Rassolov, V.; Pople, J. A. *J. Chem. Phys.* **1998**, *109*, 7764−7776.

(56) Zhao, Y.; Truhlar, D. G. *J. Phys. Chem. A* **2005**, *109*, 4209−4212.

(57) Cramer, C. J. *Essentials of Computational Chemistry*, 2nd ed; John Wiley & Sons, Ltd.: West Sussex, England, 2004; pp 165−248.

(58) Parthiban, S.; Martin, J. M. L. *J. Chem. Phys.* **2001**, *114*, 6014−6029.

(59) Helgaker, T.; Klopper, W.; Halkier, A.; Bak, K. L.; Jørgenson, P.; Olsen, J. In *Quantum Mechanical Prediction of Thermodynamic Data*; Cioslowski, J., Ed.; Understanding Chemical Reactivity; Kluwer: Dordrecht, 2001; Vol. 22, pp 1−30.

(60) Lee, T. J.; Taylor, P. R. *Int. J. Quantum Chem. Symp.* **1989**, *23*, 199−207.

(61) BS7 is not a complete basis set extrapolation because both BS5 and BS6 use the same Ru basis set, namely, the Stuttgart 1997 ECP + f. To generate a complete basis set extrapolation of extremely high accuracy, cc-pVTZ and cc-pVQZ or aug-cc-pVTZ and aug-cc-pVQZ basis sets on all atoms would be preferred; however, calculations with these basis sets are beyond our computational resources.